A Compact UWB Bandpass Filter with High Selectivity and Dual Notched-Band

Seyyed Jamal Borhani[1], M. Amin Honarvar[1], and M. Reza Namazi Rad[2]
[1]*Department of Electrical Engineering, Najafabad Branch, Islamic Azad University, Najafabad, Iran.*
[2]*SMART Infrastructure Facility, University of Wollongong, Wollongong, NSW 2522, Australia*
sj.borhani@yahoo.com, Amin.Honarvar@pel.iaun.ac.ir, mrad@uow.edu.au
[*]Corresponding author: M. Amin Honarvar

Abstract- A novel compact-sized ultra-wideband (UWB) bandpass filter (BPF) is proposed in this paper. The proposed BPF is highly selective and is able to eliminate WLAN signals from 5.15-5.35 GHz, and downlink of X-band satellite communication signals from 7.25-7.75 GHz. Generally, a multiple-mode resonator (MMR), comprised of a U-shaped line, with two high impedance stubs connected to it, and one stepped impedance resonator placed in the center of the U-shaped line is used to generate five resonate modes in the desired band (range of 3.1-10.6 GHz). Two transmission zeroes (TZs) are also placed to improve the bandage steepness. One of these TZs is with a lower cutoff frequency and the other TZ is with a higher cutoff frequency. A C-shaped open-circuited stub without adding any circuit size is parasitically coupled to the inner part of the U-shaped stub and can provide a narrow notched band at any desired frequency with appropriate bandwidth through the dimension of the parasitic element and its distance to the MMR. This C-shaped stub is used to reject WLAN signals. Furthermore, UWB passband is fully covered using asymmetric feed lines with defected interdigital coupled-lines. At the same time, another notched-band is implemented to reject X-band signals. Slots in the ground plane and input/output ports are etched to increase coupling and improve the in-band performance. The proposed BPF in the study covers UWB span completely and eliminate two bands of unwanted WLAN and X-band signals, with good linearity in the passband. A prototype filter was fabricated and its performance was measured to validate the simulation results.

Index Terms- Bandpass filter, multiple-mode resonator, dual notched-bands, ultra-wideband, WLAN, X-band satellite communication.

I. INTRODUCTION

Ultra-wideband (UWB) systems need to operate in an extremely large bandwidth from 3.1~10.6 GHz according to Federal Communication Committee (FCC) [1,2]. In such systems, to improve overall performance as a vital component bandpass filters (BPFs) with sharp rejection skirts, wide upper stopband, flat group delay variations, and compact size are highly required. On the other hand, due to the existence of some communication systems in UWB span (e.g. WiMAX (3.4-3.6 GHz), WLAN

Manuscript received 5-May-2015 and revised 26-August-2015, *P- ISSN: 2322-4088*
Accepted on 8- Nov.-2015 *E- ISSN: 2322-3936*

(5.15-5.35 and 5.725-5.825), X-band satellite communication services (downlink: 7.25-7.75 GHz, uplink: 7.9-8.395 GHz)), single or multiple notched bands must be implemented in the UWB bandwidth to avoid interference with these systems. Fulfilling these requirements is very challenging for design engineers. In [3-6], UWB passband with high selectivity using multiple-mode resonator (MMR) technique is discussed, but without notching band. Single notched band UWB BPF put forward in [7-12], with different structures. The proposed configurations in [13-17] has achieved dual notches at specific frequencies. Coupled resonator is used in [13,14] to realize notched-bands characteristic, but the UWB passband is embarrassed from poor selectivity. Notched bands at 5.3 and 7.8 GHz is created in [15]. However, the filter suffers from the problem of large circuit size. While a dual notched bands UWB BPF is proposed in [16] based on signal superposition, both size and upper stopband are to be improved. Quadruple-mode UWB BPF is discussed in [17] with high selectivity performance and notches at 5.2 and 8.05 GHz. As in [17], using short-ended stub in the structure causes fabrication complexity. Hence, there is still a necessity for a simple and compact filter with sharp rejection skirts, and notched-bands functionality to eliminate radio signals appearing in the UWB passband.

In this study, a novel microstrip-line UWB BPF based on MMR technique and manipulating interdigital-coupled lines is proposed. The MMR structure has two high impedance lines, which is tapped and connected to a U-shaped low impedance line and a stepped impedance resonator is loaded in the center of the U-shaped stub. All together this structure provides five resonate modes in the UWB passband together with two transmission zeroes (TZs) on the edge of the passband, i.e. 2.84 and 10.81 GHz, leading to a high frequency selectivity level. In this new structure, to eliminate WLAN signals at 5.25 GHz, the C-shaped open-circuited stub is utilized as a parasitically coupled element. The defected interdigital-coupled lines are formed in a way that the coupled lines are with uneven length and can transfer the discrete MMR resonate modes into an UWB passband. They can also produce second notching band at 7.5 GHz. By adjusting relevant dimensions properly, the proposed filter covers UWB span with sharp rejection skirts, wide upper stopband, and flat group delay and at the same time dual notched bands characteristic with appropriate 3-dB bandwidth. This will help to avoid signals from WLAN and downlink of X-band satellite communication systems. BPF's performance is enhanced with creating two slots in the ground plane under high impedance lines and in the input/output ports. Design and optimization of the proposed filter is carried out on RogersRO4003 substrate with relative dielectric constant $\varepsilon_r = 3.38$ thickness $h = 0.508mm$ and $\tan\delta = 0.0022$. The measured results are in good agreement with simulated predictions.

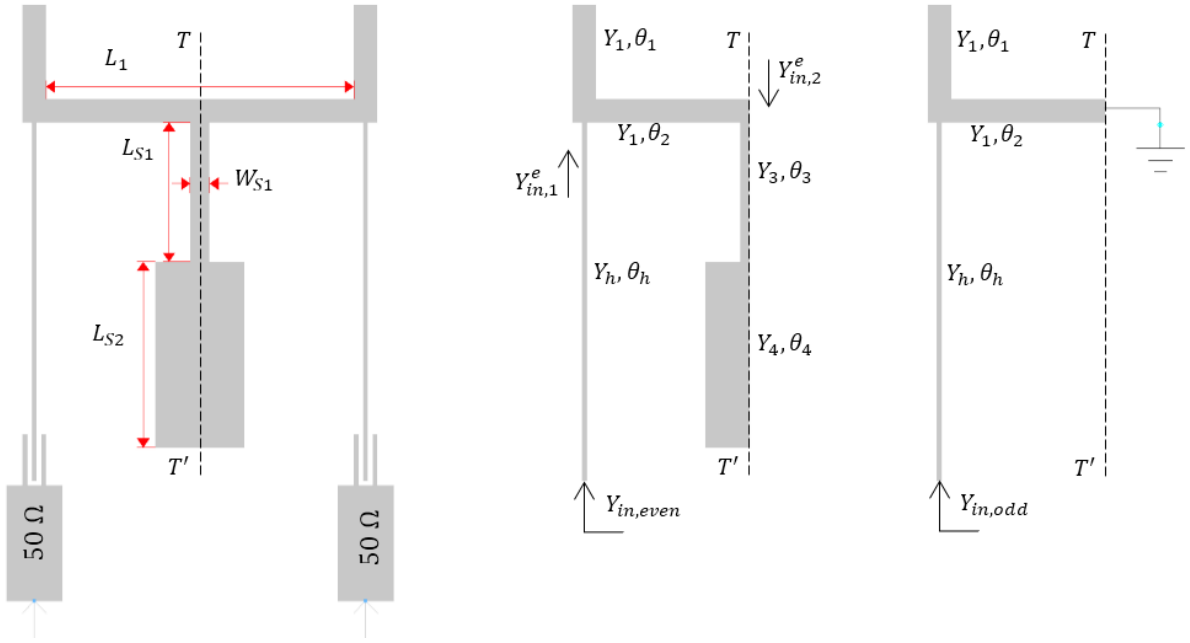

(a) (b) (c)

Fig. 1. (a) The proposed MMR structure weakly coupled with input/output feed lines. (b) Even- and (c) Odd-mode equivalent circuits.

II. PROPOSED MMR CHARACTERISTICS

Basic MMR structure of the proposed notched-band filter is shown in Fig. 1(a). It is made up of a low-impedance transmission line formed as a U-shaped stub, and two joint high-impedance lines at bottom side of the U-shaped stub. A stepped-impedance stub is located between two high-impedance lines in the center of the U-shaped stub. The lengths of the high-impedance lines and the U-shaped low-impedance line are $\lambda_g/4$ and $\lambda_g/2$, respectively. This is while λ_g is guided-wavelength with respect to the center frequency $f_0 = 6.85\,\text{GHz}$ to produce three resonate modes in the UWB passband. The stepped-impedance resonator can also generate two additional resonate modes and two TZs simultaneously to improve filter's selectivity. It will noted that, the proposed MMR structure is symmetric in structure, hence even- and odd-mode analysis method could be adopted to investigate its characteristics. The even and odd mode excitations of the resonator are presented in Fig. 1(b) and(c), respectively.

Base on the transmission line theory, the input admittances can be calculated as follows:

$$Y_{in,even} = Y_h \frac{Y^e_{in,1} + jY_h \tan\theta_h}{Y_h + jY^e_{in,1} \tan\theta_h} \tag{1}$$

Where

$$Y^e_{in,1} = jY_1 \tan\theta_1 + Y_1 \frac{Y^e_{in,2} + jY_1 \tan\theta_2}{Y_1 + jY^e_{in,2} \tan\theta_2}, \tag{2-a}$$

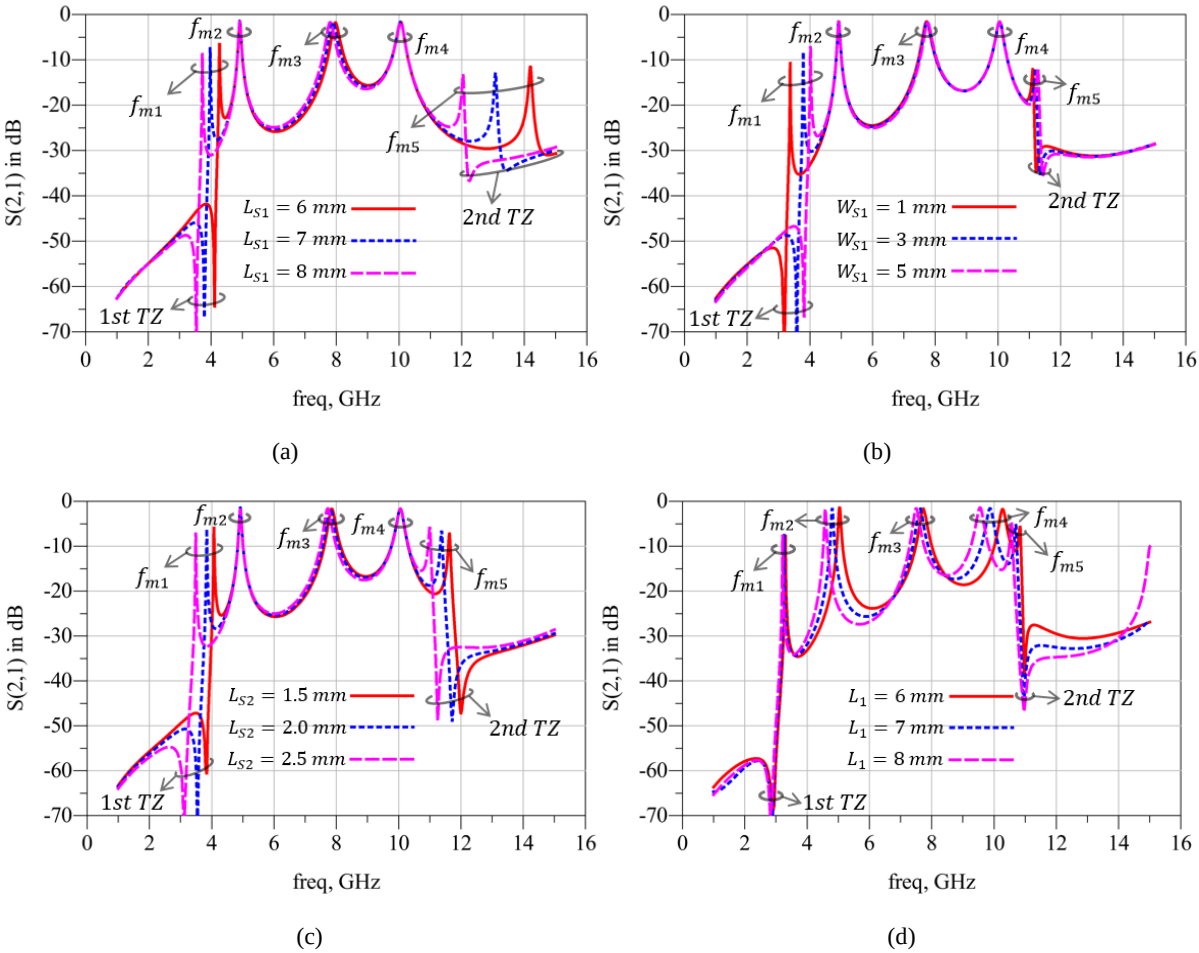

Fig. 2. Simulated $|S_{21}|$ response of the MMR with different dimensions of (a) L_{S1}, (b) W_{S1}, (c) L_{S2}, and (c) L_1.

$$Y_{in,2}^{e} = jY_3 \frac{Y_4 \tan\theta_4 + Y_3 \tan\theta_3}{Y_3 - Y_4 \tan\theta_4 \tan\theta_3}. \qquad (2\text{-b})$$

Besides,

$$Y_{in,odd} = jY_h \frac{Y_1 \tan\theta_1 \tan\theta_2 - Y_1 + Y_h \tan\theta_h \tan\theta_2}{Y_h \tan\theta_2 - Y_1 \tan\theta_1 \tan\theta_2 \tan\theta_h + Y_1 \tan\theta_h} \qquad (3)$$

From the following two conditions, $Y_{in,even} = 0$, $Y_{in,odd} = 0$, the even- and odd- resonate frequencies and by setting $Y_{in,even} = Y_{in,odd}$, TZs frequencies could be extracted.

Under weak coupling with $50\,\Omega$ input/output feed lines and by means of electromagnetic (EM) simulator software, Agilent ADS Momentum, MMR characteristics with varied $(L_{S1}, W_{S1}, L_{S2}, L_1)$ parameters as indicated in Fig. 1(a) is studied as shown in Fig. 2. It clearly can be seen that there are five resonate modes, i.e. f_{m1}, f_{m2}, f_{m3}, f_{m4}, and f_{m5} and two TZs.

In the odd mode excitation, middle plane of the MMR is short-circuited. It can be validly theorized that the central location of the resonator corresponds to a perfect electrical wall for odd modes. Consequently, the stepped-impedance open stub at the center could be ignored. Therefore

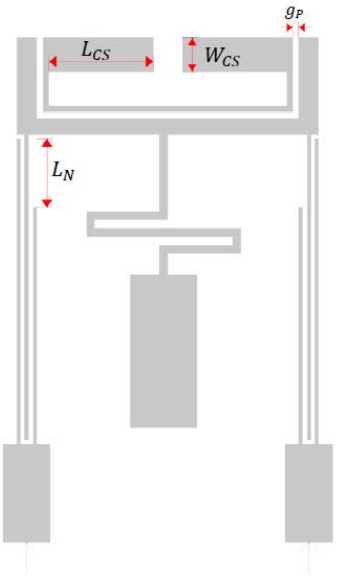

Fig. 3. Initial structure of the proposed dual notched-bands UWB BPF.

(L_{S1}, W_{S1}, L_{S2}) parameters do not impact on odd resonate modes, i.e. f_{m2}, and f_{m4}. Therefore, the even mode frequencies could be adjusted by stepped-impedance open stub while the odd modes are still unchanged. As L_{S1} changes from 6 to 8 mm, the fifth resonate mode and the second TZ shift to lower frequencies considerably. At the same time, f_{m1} and the first TZ is shifted to lower extensions. This is while the third resonate mode is being influenced to a certain level, as demonstrated in Fig. 2(a). When the width of W_{S1} increases from 1mm to 5mm (as plotted in Fig. 2(b)), f_{m1} together with the first TZ move considerably to higher frequencies, while f_{m5} and the upper TZ move slightly to higher frequencies. When the length of L_{S2} increases from 1.5mm to 2.5mm (as plotted in Fig. 2(c)), resonate modes f_{m2} and f_{m4} remain unchanged and f_{m3} changes slightly. This is while f_{m1} and f_{m5} together with both TZs can move to lower frequencies. It will be noted that, L_1 can be used for tuning odd resonance modes. As the length of L_1 increases, both f_{m2} and f_{m4} move to lower frequencies, while the movement in f_{m4} is larger than the movement in f_{m2}. As shown in Fig. 2(d) the increase in the length of L_1 has a negligible effect on f_{m1} and TZs, while f_{m3} and f_{m5} are partly affected. The results show that the proposed structure provides excellent degrees of freedom in controlling these five resonate modes to be placed in required points such that UWB passband is fully covered and the two TZs are located at the edges of the passband to improve selectivity filtering characteristic.

III. Dual Notched-Bands UWB BPF

Initial structure proposed for the compacted-sized dual notched-bands UWB BPF is shown in Fig. 3. This is designed in a way to have a single ultrawide passband obtained by incorporating five discrete resonate modes, and two inherent TZs obtained from the proposed MMR. Here, the defected

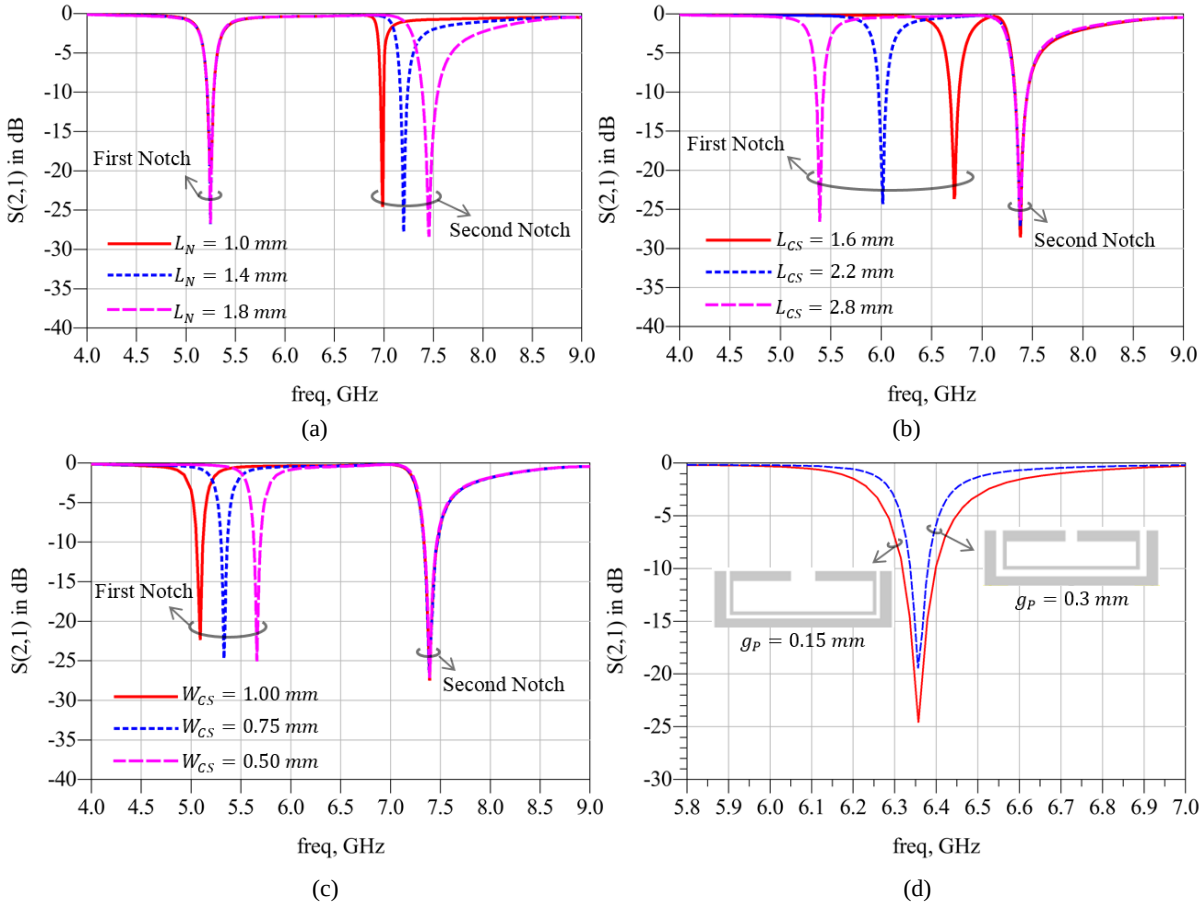

Fig. 4. Simulation results of notched-bands center frequency and their 3-dB bandwidth versus (a) L_N, (b) L_{CS}, (c) W_{CS}, and (d) g_p.

interdigital-coupled lines is employed. Unlike the conventional interdigital coupled-lines, two arms of the coupled-lines proposed in this paper are not with the same length. This means that the length of the inner lines is less than the length of the outer lines. This makes the interdigital coupled-lines to be defected. Here, the asymmetrically in the coupled-lines causes a notched-band to be implemented. The other notched-band is created with C-shaped open-circuited stub that is coupled with the inner section of the U-shaped low-impedance stub, without adding any circuit size to the MMR structure. The C-shaped open-circuited stub could be modeled as an LC circuit. On the other hand, for the fifth resonate mode and second TZ to be placed at upper cutoff frequency in a proper way, the length of the lower section of the stepped-impedance resonator should be reasonably long. Therefore, this stub is meandered to make the overall circuit size more compact.

Fig. 4 presents the results of the simulation study used in this paper to analyze the properties of modified interdigital coupled-lines with regards to the parameter L_N and the properties of C-shaped coupled stub with regards to the parameters L_{CS}, W_{CS}, and g_p on the notched bands.

The effect of L_N on central frequency of the second notch band and its 3-dB bandwidth are illustrated in Fig. 4(a), while the first notched-band does not change. When L_N increases from 1 to 1.8 mm (i.e. the length of inner lines when coupling, become smaller), the central frequency of second notched

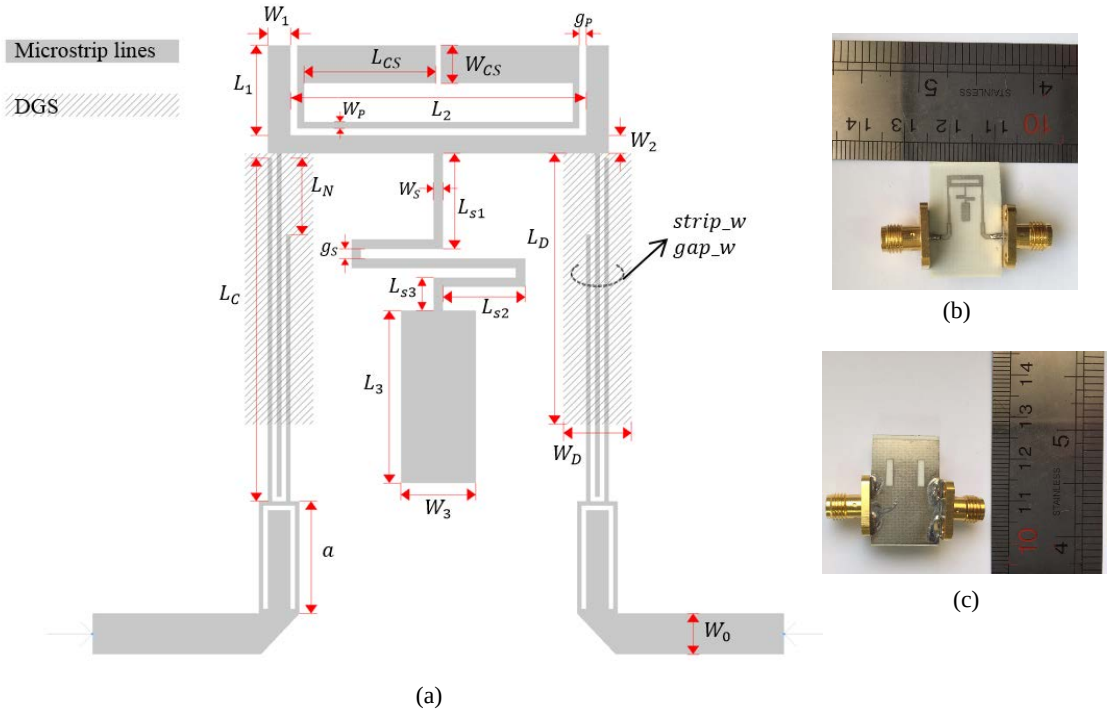

Fig. 5. (a) Final configuration of the proposed dual notched-bands filter. (b) Top view of the fabricated filter. (c) Bottom view of the fabricated filter.

band shifts to upper frequencies (i.e. from 6.99 to 7.46 GHz). This is while, the 3-dB bandwidth increases significantly (i.e. from 90 MHz to 595MHz). As shown in Fig. 4(b), for the C-shaped parasitically coupled line, an increase in L_{CS} from 1.6mm to 2.8mm, only causes changes in the frequencies of center of first notched-band and 3-dB bandwidth. This means that the center of first notched-band decreases from 6.73 GHz to 5.39 GHz, and 3-dB bandwidth becomes narrower from 270 MHz to 212 MHz. Alternatively, the width of the C-shaped stub can be also used to fine-tune the central frequency of the first notch. As shown in Fig. 4(c), when W_{CS} decreases from 1mm to 0.5mm, the central frequency of the first notch moves around 570 MHz to the upper frequencies from 5.09 GHz. For the other key degree of freedom, the space between C-shaped stub and MMR can determine the bandwidth of the notched-band, as demonstrated in Fig. 4(d). That said, when the parasitical stub has a shorter distance to the MMR, this causes a larger bandwidth for the 3-dB.

As a conclusion, with a carful and accurate adjustment in the dimensions of C-shaped coupled line and the space between the C-shaped coupled line and the resonator, a notched-band can be obtained at a specific frequency with a desired 3-dB bandwidth.

IV. Final Configuration and Discussion

Considering the numerical analysis presented in the previous sections and to validate the simulation results, a prototype of the optimized structure is fabricated and tested. The measurements were lead using Agilent network analyzer HP8722ES. The final designed configuration for the proposed dual notched-bands UWB BPF is presented in Fig. 5. Here, the U-shaped slots in the 50 Ω input/output

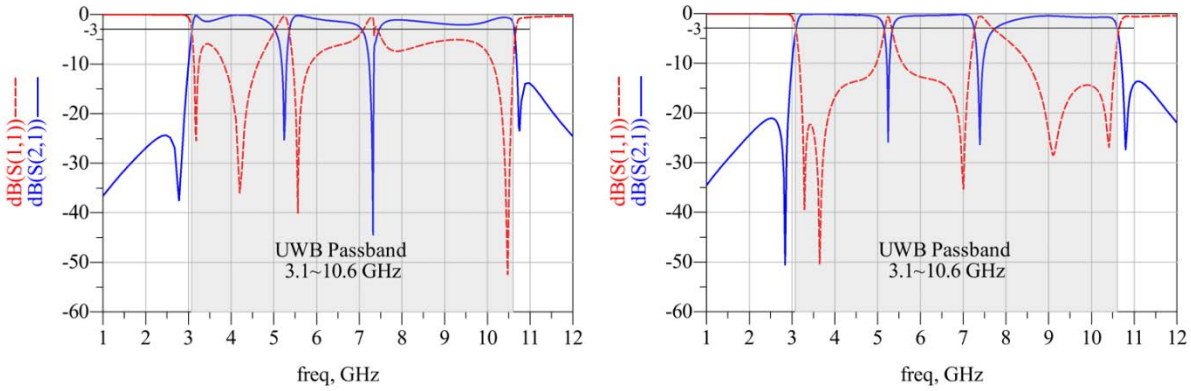

Fig. 6. Simulated S-parameters of the notched-band filter. (a) Without DGS. (b) With DGS

feed lines and defected ground structure (DGS) (as rectangular-shaped slots in the ground plane located immediately under high impedance coupling lines,) are inserted to achieve stronger coupling and therefore enhancing the passband performance. The photograph of the fabricated filter is shown in Fig. 5(b) and (c).

Using the proposed design, the optimized dimensions of the filter using EM simulator ADS are: $W_1 = 0.5$, $L_1 = 1.99$, $W_2 = 0.4$, $L_2 = 6.51$, $g_p = W_p = 0.15$, $L_{CS} = 2.9$, $W_{CS} = 0.84$, $W_S = g_S = 0.21$, $L_{S1} = 2.11$, $L_{S2} = 1.81$, $L_{S3} = 0.73$, $W_3 = 1.65$, $L_3 = 3.81$, $L_C = 7.58$, $strip\_w = gap\_w = 0.1$, $L_N = 1.69$, $W_D = 1.5$, $L_D = 5.98$, $a = 2.48$, and $W_0 = 0.9$. Note that, all units are in millimeters. The proposed filter in this paper has a compact size of $8.51\text{mm} \times 10.07\text{mm}$ (or $0.32\,\lambda_g \times 0.38\,\lambda_g$), without considering input and output ports. In a practical point of view, it will be noted that no short-circuited stub is used in the structure of the proposed filter.

Simulated S-parameters of the proposed notched-band filter with and without DGS are shown in Fig. 6. As we can observe from Fig. 6, aperture-backed coupling structure can raise the coupling degree while relaxing the line space [18].

The simulated and the measured S-parameters for the proposed filter are presented in Fig. 7. Simulated results are provided both by ADS, and HFSS. As shown in Fig. 7, there is a good level of agreement between simulation and measurement results. Small discrepancy in the results might be to non-precise SMA connector and poor soldering craft, material parameters, and also fabrication tolerance. On the other hand putting the structure in a specific box improves the insertion loss at higher frequencies, which is one of the most important reasons of the errors in the measurement results.

The 3-dB passband is exactly located between 3.1 and 10.6 GHz, i.e. bandwidth of 7.5 GHz, and central frequency at 6.85 GHz. The fractional bandwidth (FBW) is 109.49%, with all ideal UWB BPF specifications. It can be observed that, within the UWB passband, the maximum insertion loss and minimum return loss is achieved at 2.07 and ~10 dB, respectively, whereas, as compared to 0.8 and 16 dB in simulation. The filter exhibits sharp selectivity with TZs placed near the edges of the passband

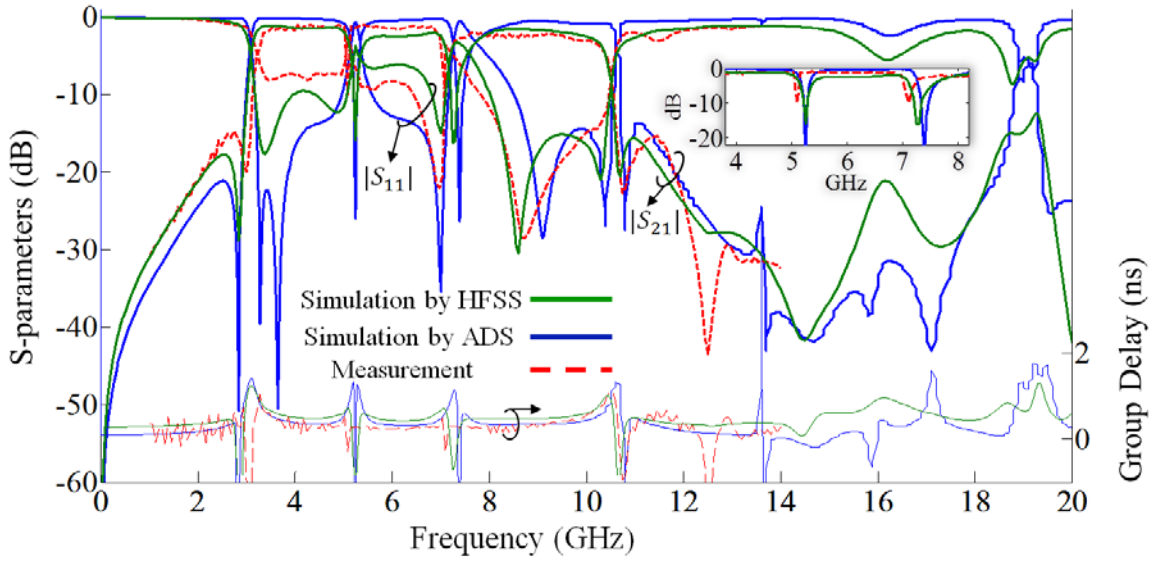

Fig. 7. Simulated and measured S-parameters and group delay of the proposed filter.

at 2.84 and 10.81 GHz in simulation and at 3.02 and 10.75 GHz in measurement. The skirt factor (*S.F.*) is used to evaluate selectivity of the filters, which could be defined as fraction of 3-dB bandwidth to 20-dB bandwidth of the passband. The *S.F.* of the proposed filter is 0.956, which is very better than the notched-band filters reported in [7-16]. Additionally, the dual narrow notched bands with different 3-dB bandwidth in the wide passband can be observed. The notched-band between 7.25 and 7.75 GHz, with a rejection level of 27.12 dB is strategically implemented with defected interdigital-coupled lines, which could effectively reject undesirable signals in downlink of X-band satellite communication system. The first notched-band is from 5.15 to 5.35 is implemented with C-shaped parasitically coupled line to reject unwanted WLAN signals, and the attenuation is around 26 dB. Simulated results by HFSS shown notched with center frequencies of 5.25, and 7.25 GHz, more than 15.8 dB attenuation level is obtained. Conclusively, reasonable bandstop characteristics for both notches are accomplished. The measured center frequency of notched band slightly shifts down from the simulated results.

A comparison of measured and simulated group delay is also shown in Fig. 7. The measured group delays within the UWB passband is about from 0.27 ns to 0.95 ns. A good linearity across the UWB passband exclude the notches can be seen in Fig. 7. The attenuation level in lower and upper stopband is more than 20 dB and 13.63 dB, respectively. Upper stopband extended to 18.8 GHz with 10 dB rejection level, wide upper stopband is obtained. Table 1 provides a comparison between key features of this work and other notched-band UWB BPFs.

Table 1: Comparison with other UWB BPFs.

Ref.		Skirt Factor	NB / Attention	f_u (GHz) / RL (dB)	Short-Circuited Stub	Size ($\lambda_g \times \lambda_g$)
[12]		0.954	5.49 / 48.33	18.76 / 20	No	0.35 × 0.37
[14]		0.751	~5.8, ~8.0 GHz / ~24, ~26 dB	14> / 30	Yes	0.93 × 0.45
[15]		0.825	5.3, 7.8 GHz / ~20, ~28 dB	~26 / 18	Yes	1.02 × 0.54
[16]		0.916	5.2, 8.9 GHz / ~34 , ~32 dB	~16.4 / 14	No	0.93 × 0.14
[17]		0.962	~5.2, ~8.05 GHz / ~34, ~22 dB	14> / 13	Yes	0.35 × 0.15
Current Design	Simulation	0.956	5.25, 7.50 GHz / 26.03, 27.12 dB	18.8 / 10	No	0.32 × 0.38
	Measurement	0.905	5.10, 7.11 GHz / 10.0, 10.1 dB	14 GHz>		

NB: notched-band(s) center frequency, f_u : upper stopband, RL: Rejection Level

V. CONCLUSIONS

A novel UWB BPF with dual notched-bands is postposed and analyzed numerically in this paper. The proposed filter is a combination of a modified MMR, a parasitic coupled C-shaped open-circuited stub without adding any circuit size, and asymmetrically feeding thru defected interdigital coupled-lines to a UWB filter with dual notched bands functionality with different 3-dB bandwidth to be achieved. UWB passband with five resonate modes of the proposed MMR and two TZs of it with high selectivity is completely covered, and with manipulating interdigital coupled-lines one notched band is implemented at downlink of X-band satellite communication from 7.25-7.75 GHz. The dimension of the C-shaped and its distance to the MMR is carefully tuned to generate a narrow notch from 5.15-5.35 GHz for avoiding WLAN signals. While the proposed notched-band filter is simplified, it is relatively flexible to UWB where the passband is entirely covered, and the undesirable WLAN and X-band signals are rejected. It also has a compact size of 8.51mm×10.07mm and high frequency selectivity with skirt factor of 0.956, which all these attributes made the proposed filter attractive for a practical point of view.

REFERENCES

[1] FCC, Revision of Part 15 of the Commission's Rules Regarding Ultra-Wideband Transmission System, Washington, DC, ET- Docket 98–153, Feb. 2002.

[2] M. Majidzadeh, Ch. Ghobadi, and J. Nourinia, Compact CPW-fed Circular Patch Antenna for UWB Applications," *Journal of Communication Engineering*, vol. 2, no.1 , pp. 63-72, Winter 2013.

[3] Q.-X. Chu, X.-H. Wu, and X.-K. Tian, "Novel UWB Bandpass Filter Using Stub-Loaded Multiple-Mode Resonator," *IEEE Microw. Wireless Compon. Lett.*, vol. 21, no. 8, pp. 403-405, Aug. 2011.

[4] Z. Zhang and F. Xiao, "An UWB Bandpass Filter Based on a Novel Type of Multi-Mode Resonator," *IEEE Microw. Wireless Compon. Lett.*, vol. 22, no. 10, pp. 506-508, Oct. 2012.

[5] Z. Shang, X. Guo,B. Cao, B. Wei, X. Zhang, Y. Heng, G. Suo, and X. Song, "Design of a Superconducting Ultra-Wideband (UWB) Bandpass Filter With Sharp Rejection Skirts and Miniaturized Size," *IEEE Microw. Wireless Compon. Lett.*, vol. 23, no. 2, pp. 72-74, Feb. 2013.

[6] S. J. Borhani and M. A. Honarvar, "A Novel Compact Size UWB Bandpass Filter with Sharp Rejection Skirt and Wide Upper-Stopband Based on Multiple-Mode-Resonator," *Progress In Electromagnetics Research C*, vol. 43, pp. 175-185, 2013.

[7] S. W. Wong, and L. Zhu, "Implementation of Compact UWB Bandpass Filter With a Notch-Band," *IEEE Microw. Wireless Compon. Lett.*, vol. 18, no. 1, pp. 10-12, Jan. 2008.

[8] S. Pirani , J. Nourinia, and C. Ghobadi, "Band-Notched UWB BPF Design Using Parasitic Coupled Line," *IEEE Microw. Wireless Compon. Lett.*, vol. 20, no. 8, pp. 444-446, Aug. 2010.

[9] M. A. Honarvar and R. A. Sadeghzadeh, "Design of Coplanar Waveguide Ultrawideband Bandpass Filter Using Stub-Loaded Resonator with Notched Band," *Microwave Opt. Technol. Lett.*, vol. 54, no. 9, pp. 2056-2061, Sep. 2012.

[10] H. Zhu, and Q.-X. Chu, "Ultra-Wideband Bandpass Filter With a Notch-Band Using Stub-Loaded Ring Resonator," *IEEE Microw. Wireless Compon. Lett.*, vol. 23, no. 7, pp. 341-343, Jul. 2013.

[11] Q. Yi, M. Zhang, F. Zhou, and X. Luo, "An Ultrawideband Single Notched-Band Bandpass Filter by Consisting of CRLH TL and EOS," *Microwave Opt. Technol. Lett.*, vol. 56, no. 5, pp. 1115–1118, May 2014.

[12] S. J. Borhani, M. A. Honarvar, and B. S. Virdee, "High selectivity UWB bandpass filter with a wide notched-band," *Microwave Opt. Technol. Lett.*, vol. 57, no. 3, pp. 634-639, March 2015.

[13] Feng Wei, Lei Chen, Zhu Dan Wang and Xiao Wei Shi, "Ultra-Wideband Band-Pass Filter with Dual Narrow Notched Bands based on Dual-Mode Stepped Impedance Resonator," *Microwave Opt. Technol. Lett.*, vol. 55, no. 4, pp. 727–730, Apr. 2013.

[14] J. Zhao, J. Wang, G. Zhang, and JL Li , "Compact Microstrip UWB Bandpass Filter With Dual Notched Bands Using E-Shaped Resonator," *IEEE Microw. Wireless Compon. Lett.*, vol. 23, no. 12, pp. 638-640, Dec. 2013.

[15] Y. H. Song, G. M. Yang, and W. Geyi, "Compact UWB Bandpass Filter With Dual Notched Bands Using Defected Ground Structures," *IEEE Microw. Wireless Compon. Lett.*, vol. 24, no. 4, pp. 230-232, Apr. 2014.

[16] M. Mirzaee, S. Noghanian, and B. S. Virdee, "High Selectivity UWB Bandpass Filter with Controllable Bandwidth of Dual Notch Bands," *Electron. Lett.*, vol. 50, no. 19, pp. 1358–1359, Sep. 2014.

[17] P. Sarkar, R. Ghatak, M. Pal, and D. R. Poddar , "High-Selective Compact UWB Bandpass Filter With Dual Notch Bands," *IEEE Microw. Wireless Compon. Lett.*, vol. 24, no. 7, pp. 448-450 , Jul. 2014.

[18] L. Zhu, H. Bu, and K. Wu, “Broadband and compact multi-pole microstrip bandpass filters using ground plane aperture technique,” *Proc. Inst. Elect. Eng.*, vol. l49, no. 1, pp. 71–77, 2002.